

Evidence for an unusual dynamical-arrest scenario in short-ranged colloidal systems

G. Foffi,¹ K. A. Dawson,¹ S. V. Buldyrev,^{2,3} F. Sciortino,² E. Zaccarelli,² and P. Tartaglia²

¹*Irish Centre for Colloid Science and Biomaterials, Department of Chemistry, University College Dublin, Belfield, Dublin 4, Ireland*
²*Dipartimento di Fisica, Istituto Nazionale di Fisica della Materia, and INFM, Center for Statistical Mechanics and Complexity, Università di Roma "La Sapienza," Piazzale Aldo Moro 5, I-00185 Rome, Italy*

³*Center for Polymer Studies and Department of Physics, Boston University, Boston, Massachusetts 02215*

(Received 21 January 2002; published 21 May 2002)

Extensive molecular dynamics simulation studies of particles interacting via a short-ranged attractive square-well potential are reported. The calculated loci of constant diffusion coefficient D in the temperature-packing fraction plane show a reentrant behavior, i.e., an increase of diffusivity on cooling, confirming an important part of the high volume-fraction dynamical-arrest scenario earlier predicted by theory for particles with short-ranged potentials. The more efficient localization mechanism induced by the short-range bonding provides, on average, additional free volume as compared to the hard-sphere case and results in faster dynamics.

DOI: 10.1103/PhysRevE.65.050802

PACS number(s): 82.70.Dd, 83.80.Hj, 61.12.Ex, 61.25.Hq

Recently a large number of novel dynamical-arrest phenomena have been described in systems where, besides the usual hard core, an attractive potential is present with a range much smaller than the hard-core radius [1–3]. This condition is not usually met in molecular liquid systems, where the attractive range is of the same order of magnitude as the hard core, but can be realized in colloidal systems where the size of the particles largely exceeds the range of the attractive part of the potential [4–8], and possibly many other systems of experimental interest, including globular proteins [9,10]. From the experimental point of view the most striking phenomenon associated with the attraction is the gradual disappearance of the liquid phase when the range of the attractive part of the potential diminishes. Ultimately, for narrower wells, the liquid-gas coexistence becomes metastable with respect to a crystal-fluid equilibrium, but nevertheless shows up as a metastable binodal curve in experiments [8] and in simulations [11]. Various approximations to the liquid and crystalline free energies have been used in order to calculate the coexistence lines and for various forms of the attractive part of the interaction potential [12–15].

While the situation of the equilibrium phase diagram is quite clear, the metastable region of the phase diagram related to the supercooled fluid is quite complex, and only partially clarified [8,16,17]. It is now widely accepted that mode-coupling theory (MCT) provides a description of supercooled dynamics that is particularly suitable for understanding colloidal systems. MCT predicts, in particular, the existence of a nonergodicity transition that corresponds to a structural arrest, i.e., the impossibility of the particles of the system to move under the effect of the neighboring ones, the so-called cage effect [18,19]. Some measurements performed in colloidal systems support the MCT predictions in more quantitative detail [20,21]. More recently MCT has been applied to systems interacting through a short-ranged attractive potential, with the result of predicting a number of new and interesting phenomena [1,2,22,23]. Among the most striking is the possibility of distinguishing two types of transitions from a supercooled liquid to a glass, one mainly due to the repulsive part of the potential through the usual mechanism

of the cage effect, the other to the attractive part of the potential. The latter mechanism is due to the adhesiveness of the potential at short distances that produces “clusters” of particles, a different mechanism of structural arrest than the “blocking” or “jamming” familiar in hard-sphere systems. The attractive branch of glass transition curve that results extends from low values of the volume fraction ϕ to values of the order of the hard-sphere transition and does not vary much with temperature. The repulsive glass curve passes from the hard-sphere value at high temperatures to larger values of ϕ as temperature decreases, thereby giving rise to a reentrant phenomenon, i.e., the supercooled liquid phase extends into the glass region above the volume fractions of the pure hard-spheres system. It is then possible, raising the temperature at constant volume fraction, to move from the attractive glass region to the supercooled fluid one and again in the amorphous hard-sphere-like glass region. We note in passing that the complementary possibility of driving the system across a glass transition both by increasing and decreasing the density has been shown to be possible in systems with long-range interactions (Wigner glasses) [24]. Here in the case under scrutiny, at high values of ϕ , the two branches of the glass curves cross at an angle, and the attractive branch continues further into the glass region, giving rise to a remarkable coexistence of two different types of glass that can be characterized, for example, by their mechanical properties such as the shear modulus [25]. The glass-glass curve terminates in a special singular point of the theory, named A_3 in the MCT, where the relaxation processes have a peculiar behavior [26]. Upon narrowing the width of the attractive potential, the glass-glass transition line tends to become shorter until it vanishes in a point that represents a high order singularity, an A_4 singularity in the MCT language [22]. The experimental and/or numerical verifications of these predictions are still scarce [6,23]. A logarithmic decay, predicted by MCT close to the A_3 point, was detected, in particular, in a micellar system at high packing fractions [27]. It is interesting to note the possible application of this type of results to the study of protein crystallization [9,15].

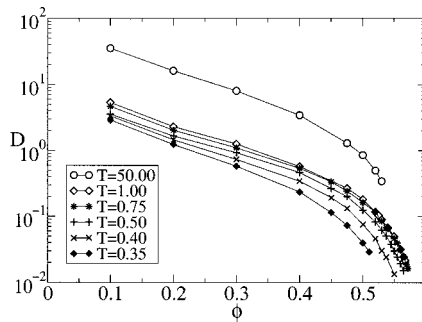


FIG. 1. Diffusion coefficient D as a function of the packing fraction ϕ for the $\epsilon=0.03$ square-well potential at several different T .

We focus in this paper on a particular aspect of the attractive colloidal system, that is the extension of the glass transition line to high values of the packing fraction, in order to test one of the important predictions of the theory, i.e., the reentrant behavior of the supercooled fluid-glass line. We simulate a monodisperse sample of $N=1237$ particles of unit mass with a constant diameter $\sigma=1$ in a cubic box. The physical quantities are measured in units of the particle diameter σ , the particle mass m , and the square-well (SW) depth u_0 as unit of energy. Temperature T is measured in units of energy, i.e., by setting the Boltzmann constant $k_B=1$. With these choices, time is measured in units of $\sigma(m/u_0)^{1/2}$. The interparticle potential $V(r)$ is the square-well potential,

$$\begin{aligned} V(r) &= \infty, & r < \sigma \\ V(r) &= -u_0, & \sigma < r < \sigma + \Delta \\ V(r) &= 0, & r > \sigma + \Delta. \end{aligned} \quad (1)$$

The width of the attractive part of the potential is $\Delta=0.0309$, corresponding to a percentage variation $\epsilon=\Delta/(\sigma+\Delta)=0.03$. We have investigated volume fractions from 0.10 to ≈ 0.58 and temperatures from $T=0.32$ to 50. For T lower than 0.32 the homogeneous fluid phase is unstable with respect to gas-liquid phase separation. MCT calculations, based both on the Percus-Yevick and mean spherical approximation structure factors [22], predict, for this specific potential, a reentrant fluid-glass line, as discussed in what follows. We have implemented the standard molecular dynamics algorithm for particles interacting with SW potentials [28]. Between collisions, particles move along straight lines with constant velocities. When the distance between the particles becomes equal to the distance for which $V(r)$ has a discontinuity, the velocities of the interacting particles instantaneously change. The algorithm calculates the shortest collision time in the system and propagate the trajectory from one collision to the next one. Calculations of the next collision time are optimized by dividing the system into small subsystems, so that collision times are computed only between particles in the neighboring subsystems.

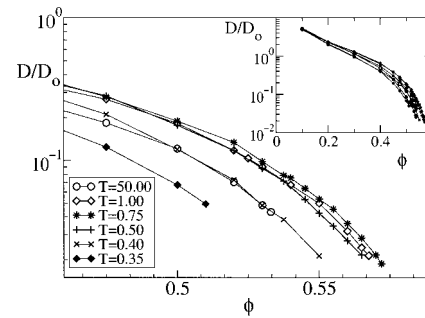


FIG. 2. Scaled diffusivity D/D_0 [$D_0=\sigma(T/m)^{0.5}$] as a function of packing fraction ϕ for the SW potential for some of the isotherms studied. The inset shows an enlarged ϕ window to highlight the common low density limit.

For each run we have used particular care in equilibrating the system, and starting from an equilibrated configuration we have performed a simulation up to a time 10^3 . Runs exhibiting the presence of a crystalline nucleus at the end of the simulations were discarded. Since we simulate a monodisperse system, the formation of a crystal phase fixes the range of packing fractions where a stable (or metastable) fluid phase can be studied.

We have calculated the self-diffusion coefficient D in the supercooled liquid phase via the long time limit of the mean squared displacement of the particles. For each of the ten studied isotherms, D varies almost over three decades, showing a marked decrease at high volume fractions, before crystallization takes place.

Figure 1 shows the diffusion coefficient D as a function of the packing fraction $\phi \equiv N\pi\sigma^3/(6V)$ for the studied isotherms. The $T=50$ isotherm diffusivity reproduces the hard-sphere behavior. For each isotherm, simulations at larger volume fraction than the ones reported inevitably lead to crystallization during the run. Figure 1 shows that, when the kinetic energy is of the order of the potential depth (e.g., $T=0.75$), crystallization is shifted to larger packing fraction values as compared to both the hard-sphere case (e.g., $T=50$) and to low T (e.g., $T=0.35$).

Figure 2 shows the diffusivity behavior in the ϕ region where the reentrant phenomenon takes place. Data are normalized by $D_0 \equiv \sigma\sqrt{T/m}$, in order to take into account the T dependence of the microscopic time.

We see that on decreasing T at constant ϕ , D/D_0 first increases and then decreases again. Since the $T^{1/2}$ term in D_0 accounts already for the slowing down of the dynamics associated to the different average particle velocity, the increase of D/D_0 on cooling must have a different origin. This peculiar feature can be explained as a result of the competition between two different dynamical features produced by the increased bonding: (i) slowing down of the dynamics due to the formation of a larger number of bonded pairs and (ii) speeding up of the dynamics due to the larger free volume resulting from the more efficient packing of the bonded particles—whose nearest neighbor distance is now imposed by the short range of the potential. The inset of Fig. 2 shows all the studied state points. At all T , the low density limit

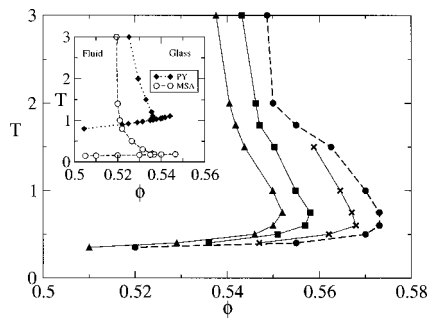


FIG. 3. Isodiffusivity curves in the (ϕ, T) phase diagram with $D/D_0 = 0.05$ (triangles), 0.04 (squares), 0.025 (crosses). The dashed line with filled circles represents the line where the system crystallizes within our maximum simulation time. The inset shows the theoretical MCT prediction for the ideal glass line (redrawn from Ref. [22]) for both Percus-Yevick (PY, filled diamonds) and mean spherical approximation (MSA, open circles), separating the fluid phase from the glass phase.

coincides with the hard sphere behavior.

Figure 3 reports the isodiffusivity curves, i.e., curves at constant D/D_0 value, in the (ϕ, T) plane. It also reports the curve where crystallization takes place within the time of our calculation. The isodiffusivity curves shown in Fig. 3 can be considered as the precursor of the fluid-glass transition line that would take place when $D/D_0 \rightarrow 0$ if crystallization would not occur first. We considered as having crystallized those configurations which, by looking at positions of particles in real space, showed evidence of nonlocal order. The inset of Fig. 3 shows the MCT calculations for the same

model as reported in Ref. [22]. As in all cases studied previously, the MCT calculation underestimates the location of the glass transition line but provides a correct frame for understanding the reentrant behavior observed in the present calculations.

In summary, we have established the presence of reentrance in the dynamical-arrest behavior of an extremely simple model, the square well one, when the width of the attractive potential is much smaller than the hard-core radius. This condition can be met in colloidal systems. This observed behavior, predicted by MCT, along with a number of other associated phenomena, is explained as competition between the hard-core caging—characteristic of the hard-core systems—and the bonding caging which, in the case of very short-range potential, localizes the particles in a more efficient manner than the hard core case. This stronger localization, imposed by incipient “bonding” provides extra free volume that leads to more diffusional pathways. Further lowering of the temperature produces stronger cages, and the system then crosses over to the attractive glass scenario. It is an open challenge to find out in future if other MCT predictions are supported by numerical investigation. This additional work, which requires the study of larger values of ϕ and larger simulation time windows to better characterize the slow dynamics—based on SW binary mixture systems to prevent crystallization—is underway.

This research was supported by the INFM-HOP-1999, MURST-PRIN-2000, and COST P1. S.B. thanks the University of Rome and NSF, Chemistry Division (Grant No. CHE-0096892) for support.

-
- [1] L. Fabbian, W. Götze, F. Sciortino, P. Tartaglia and F. Thiery, *Phys. Rev. E* **59**, R1347 (1999); **60**, 2430 (1999).
- [2] J. Bergenholtz and M. Fuchs, *Phys. Rev. E* **59**, 5706 (1999).
- [3] G. Foffi, E. Zaccarelli, F. Sciortino, P. Tartaglia, and K.A. Dawson, *J. Stat. Phys.* **100**, 363 (2000).
- [4] H.N.W. Lekkerkerker, W.C. Poon, P.N. Pusey, A. Stroobants, and P.B. Warren, *Europhys. Lett.* **20**, 559 (1992).
- [5] P.N. Pusey, A.D. Pirie, and W.C.K. Poon, *Physica A* **201**, 322 (1993); P.N. Pusey, P.N. Segrè, O.P. Behrend, S.P. Meeker, and W.C.K. Poon, *ibid.* **235**, 1 (1996); W.C.K. Poon, *Curr. Opin. Colloid Interface Sci.* **3**, 593 (1998).
- [6] E. Bartsch, M. Antonietti, W. Shupp, and H. Sillescu, *J. Chem. Phys.* **97**, 3950 (1992).
- [7] E. Bartsch, V. Frenz, J. Baschnagel, W. Schärftl, and H. Sillescu, *J. Chem. Phys.* **106**, 3743 (1997); A. Kasper, E. Bartsch, and H. Sillescu, *Langmuir* **14**, 5004 (1998).
- [8] H. Verduin and J.K.G. Dhont, *J. Colloid Interface Sci.* **172**, 425 (1995).
- [9] R. Piazza, *Curr. Opin. Colloid Interface Sci.* **5**, 38 (2000); M. Mushol and F. Rosenberg, *J. Chem. Phys.* **103**, 10 424 (1995); D.F. Rosebaum, A. Kulkarni, S. Ramakrishnan, and C.F. Zukoski, *ibid.* **111**, 9882 (1999).
- [10] M.H.J. Hagen, E.J. Mejer, G. Mooji, D. Frenkel, and H.N.W. Lekkerkerker, *Nature (London)* **365**, 425 (1993).
- [11] S. Auer and D. Frenkel, *Nature (London)* **409**, 1020 (2001).
- [12] J.A. Barker and D.J. Henderson, *J. Chem. Phys.* **47**, 2856 (1967).
- [13] A.P. Gast, W.B. Russell, and C.K. Hall, *J. Colloid Interface Sci.* **96**, 1977 (1983); **109**, 161 (1986).
- [14] M. Dijkstra, J.M. Brader, and R. Evans, *J. Phys.: Condens. Matter* **11**, 10 079 (1999).
- [15] G. Foffi, G.D. McCullagh, A. Lawlor, E. Zaccarelli, K.A. Dawson, F. Sciortino, P. Tartaglia, D. Pini, and G. Stell, *Phys. Rev. E* **65**, 031407 (2002).
- [16] P.N. Segrè, V. Prasad, A.B. Schofield, and D.A. Weitz, *Phys. Rev. Lett.* **86**, 6042 (2000).
- [17] G.F. Wang and S.K. Lai, *Phys. Rev. Lett.* **82**, 3645 (1999).
- [18] W. Götze, in *Liquids, Freezing and the Glass Transition*, edited by J.P. Hansen, D. Levesque, and J. Zinn-Justin (North-Holland, Amsterdam, 1991), p. 287.
- [19] W. Götze and L. Sjögren, *Rep. Prog. Phys.* **55**, 241 (1992).
- [20] W. Götze, *J. Phys.: Condens. Matter* **11**, A1 (1999).
- [21] W. van Meegen and S.M. Underwood, *Phys. Rev. Lett.* **70**, 2766 (1993); *Phys. Rev. E* **49**, 4206 (1994).
- [22] K.A. Dawson, G. Foffi, M. Fuchs, W. Götze, F. Sciortino, M. Sperl, P. Tartaglia, Th. Voigtmann, and E. Zaccarelli, *Phys. Rev. E* **63**, 011401 (2000).
- [23] A.M. Puertas, M. Fuchs, and M.E. Cates, *Phys. Rev. Lett.* **88**, 098301 (2002).

- [24] J. Bosse and S.D. Wilke, *Phys. Rev. Lett.* **80**, 1260 (1998).
- [25] E. Zaccarelli, G. Foffi, P. Tartaglia, F. Sciortino, and K.A. Dawson, *Phys. Rev. E* **63**, 031501 (2001).
- [26] L. Sjögren, *J. Phys.: Condens. Matter* **3**, 5023 (1991).
- [27] F. Mallamace, P. Gambadauro, N. Micali, P. Tartaglia, C. Liao, and S.H. Chen, *Phys. Rev. Lett.* **84**, 5431 (2000).
- [28] D.C. Rapaport, *The Art of Molecular Dynamic Simulation* (Cambridge University Press, Cambridge, England, 1995).